Critical exponents at the unconventional disorder-driven transition in a Weyl semimetal

S. V. Syzranov,[1,2] P. M. Ostrovsky,[3,4] V. Gurarie,[1,2] and L. Radzihovsky[1,2,5]
[1]*Physics Department, University of Colorado, Boulder, Colorado 80309, USA*
[2]*Center for Theory of Quantum Matter, University of Colorado, Boulder, Colorado 80309, USA*
[3]*Max Planck Institute for Solid State Research, Heisenbergstr. 1, 70569 Stuttgart, Germany*
[4]*L.D. Landau Institute for Theoretical Physics RAS, 119334 Moscow, Russia*
[5]*JILA, NIST, University of Colorado, Boulder, Colorado 80309, USA*
(Received 27 December 2015; revised manuscript received 10 March 2016; published 7 April 2016)

Disordered noninteracting systems in sufficiently high dimensions have been predicted to display a non-Anderson disorder-driven transition that manifests itself in the critical behavior of the density of states and other physical observables. Recently, the critical properties of this transition have been extensively studied for the specific case of Weyl semimetals by means of numerical and renormalisation-group approaches. Despite this, the values of the critical exponents at such a transition in a Weyl semimetal are currently under debate. We present an independent calculation of the critical exponents using a two-loop renormalization-group approach for Weyl fermions in $2-\varepsilon$ dimensions and resolve controversies currently existing in the literature.

DOI: 10.1103/PhysRevB.93.155113

I. INTRODUCTION

It was proposed [1,2] 30 years ago that three-dimensional (3D) disordered systems with Weyl and Dirac quasiparticle dispersion can display an unconventional disorder-driven transition that lies in a non-Anderson universality class. In particular, in contrast with the Anderson localization transition, the density of states at this transition has been suggested [1] to display a critical behavior, with the scaling function proposed in Ref. [3].

Recently, we have demonstrated [4,5] that such transitions occur near nodes and band edges in *all* materials in sufficiently *high dimensions* d and are not unique to Dirac (Weyl) systems. In systems that allow for localization the transition manifests itself also in the unusual behavior of the mobility threshold [5]. As the concept of high dimensions here is defined relative to the quasiparticle dispersion, possible playgrounds include a number of systems in physical $d = 1,2,3$ dimensions, with higher dimensions being accessible numerically. For example, recently, we have shown how this transition can be observed in 1D and 2D arrays of ultracold ions in optical or magnetic traps [6].

Because Weyl semimetals (WSMs) are currently one of the most well-known and experimentally accessible platforms [7–9] for the observation of these high-dimensional disorder-driven phenomena, tremendous research efforts have been directed at studying the critical properties of the transition in a WSM. Nevertheless, the values of the critical exponents at the transition are currently under debate.

Quantum criticality near the transition has been studied analytically for Dirac and Weyl particles in dimensions $d > 2$ by means of perturbative renormalisation-group approaches [4,5,10,11], large-N (large number of valleys or particle flavours) analysis [12], and (uncontrolled) self-consistent Born approximation [1,13,14] (SCBA), equivalent to a large-N calculation in the limit $N = \infty$.

Usually, Weyl and Dirac materials have only several nodes, $N \sim \mathcal{O}(1)$, which makes large-N approaches quantitatively inaccurate in all dimensions d [for detailed criticism of the SCBA versus RG see Refs. [4,15,16] (although Refs. [15,16] are devoted to graphene, their arguments apply as well to Dirac and Weyl particles in all dimensions)].

Perturbative renormalization-group (RG) analyses are controlled by the small parameter $\varepsilon = 2 - d$. Although such RG analysis for small ε is not guaranteed to be quantitatively accurate when analytically continued to 3D ($\varepsilon = -1$), already the one-loop results [4,5,10,11] predict the correlation-length exponent $\nu = 1$ and the dynamical exponent $z = 3/2$ that lie within 15% and several percent of the values obtained numerically in Refs. [3,17,18].

Also, numerical analysis of Ref. [6], albeit carried out for 1D chiral systems, suggest that one-loop RG results accurately describe the critical properties of such type of transitions. Recently, a value of $z = 1.49 \pm 0.02$ very close to the one-loop result $z = 3/2$ has been obtained numerically in Ref. [19]. However, the same simulations found a value of $\nu = 1.47 \pm 0.03$ very different from the one-loop prediction $\nu = 1$. It has been argued in Ref. [20] that the one-loop result $z = 3/2$ for the dynamical critical exponent is exact and holds in all orders of the renormalization, in contradiction with the analytical two-loop calculations of Ref. [11] predicting[1] $\nu = [-\varepsilon - \frac{\varepsilon^2}{8} + \ldots]^{-1} \approx 1.14$ and $z = 1 - \frac{\varepsilon}{2} - \frac{3}{16}\varepsilon^2 + \ldots \approx 1.31$. Similar analytical two-loop RG calculations for graphene [21] and for related the Gross-Neveu model [22–27], with the results for the latter being well established in the high-energy literature, yield beta functions inconsistent with those of Refs. [11,20].

In this paper, we present an independent calculation of the critical exponents for the transition in a Weyl semimetal using a two-loop renormalization group approach for Weyl fermions in $2-\varepsilon$ dimensions and resolve controversies currently existing in the literature. We obtain beta functions consistent with those obtained for graphene in Ref. [21] and for Gross-Neveu model

[1]We note that in Ref. [11] the parameter ε is defined as $\varepsilon = d - 2$, while our convention in this paper is $\varepsilon = 2 - d$.

in Refs. [22–27], but in disagreement with the results of Refs. [11,20]. We find the critical exponents to be

$$\nu = \left(-\varepsilon + \frac{\varepsilon^2}{2} + \dots \right)^{-1}, \tag{1}$$

$$z = 1 - \frac{\varepsilon}{2} - \frac{\varepsilon^2}{8} + \dots . \tag{2}$$

For a 3D Weyl semimetal ($\varepsilon = -1$), Eqs. (1) and (2) give

$$\nu \approx 0.67, \quad z \approx 1.4. \tag{3}$$

We emphasize, however, that higher-loop corrections for $\varepsilon = -1$ will lead to deviations from these values obtained from an RG calculation controlled by small ε.

II. MODEL

The critical density of states in a WSM with short-range-correlated disorder can be described in the supersymmetric representation [28] by a field theory with the action

$$\mathcal{L} = -i \int \Phi^\dagger [i\omega - \hat{\boldsymbol{\sigma}}\hat{\mathbf{k}}]\Phi \, d\mathbf{r} + \frac{1}{2}\varkappa_0 \int (\Phi^\dagger \Phi)^2 d\mathbf{r}, \tag{4}$$

where $\Phi = (\chi \; s)^T$ is a vector consisting of an anticommuting (fermionic) χ and commuting s (bosonic) components, $\omega > 0$ is the Matsubara frequency in the upper half-plane, $\hat{\boldsymbol{\sigma}}$ is a vector of matrices generating a d-dimensional Clifford algebra ($\{\hat{\sigma}_\alpha, \hat{\sigma}_\beta\} = 2\delta_{\alpha\beta}\mathbb{1}$), $\mathbf{k} = -i\boldsymbol{\nabla}$ is the momentum operator, and $\varkappa_0 = \int < U(\mathbf{r})U(\mathbf{r}') >_{\text{dis}} d\mathbf{r}'$ is the strength of the short-range-correlated random disorder potential under consideration. Equivalent field theories can be derived also in Keldysh [29] and replica [30] representations.

We emphasise, that we express the action (4) in terms of a positive Matsubara frequency ω, in contrast with the conventional real-frequency representation [28], in order to regularize integrals in the renormalization scheme used below. Also, frequency ω in Eq. (4) plays the same role as the mass m in the related Gross-Neveu model [23–25]. The density of states is determined by the retarded Green's function $G^R(E,\mathbf{r},\mathbf{r}')$ that can be obtained from the action (4) using analytic continuation to real frequencies $i\omega \to E + i0$.

We note, that realistic materials always have an even number of Weyl nodes, due to the fermion doubling theorem [31], and thus in general should be described by an action with an even number of Weyl fermion flavours. However, for sufficiently smooth disorder internodal scattering can be neglected, and the material is equivalent to an even number of copies of single-node WSMs described by the action (4).

III. RENORMALIZATION

In dimensions $d > 2$, this field theory leads to ultraviolet divergencies in physical observables and requires an appropriate RG treatment. We study the behavior of the system at frequency ω and at long length scales, $\mathbf{k} \to 0$, following the *minimal subtraction* renormalization scheme [32]. We use dimensional regularization by computing observables in lower $d = 2 - \varepsilon$ dimensions (with small $\varepsilon > 0$) and then analytically continue renormalized observables to the higher dimensions of interest ($\varepsilon < 0$). The Lagrangian (4) in this scheme is separated into the effective Lagrangian $\mathcal{L}_E$ of variables observable in the long-wave limit of interest and the counterterms:

$$\mathcal{L} = \mathcal{L}_E + \mathcal{L}_{\text{counter}}, \tag{5}$$

$$\mathcal{L}_E = -i \int \psi^\dagger (i\Omega - \hat{\boldsymbol{\sigma}}\hat{\mathbf{k}})\psi \, d\mathbf{r} + \frac{1}{2}\varkappa \int (\psi^\dagger \psi)^2 d\mathbf{r}, \tag{6}$$

where the energy scale Ω and the renormalized disorder strength $\varkappa$ are experimentally observable, and the counterterms $\mathcal{L}_{\text{counter}}$ cancel the divergent (in the powers of $1/\varepsilon$) contributions to physical observables that come from the Lagrangian (6).

The strength of disorder can be conveniently characterized by the dimensionless parameter [5]

$$\gamma = 2C_d \varkappa \, \Omega^{-\varepsilon}, \tag{7}$$

where $C_d = 2^{1-d}\pi^{-\frac{d}{2}}/\Gamma(\frac{d}{2})$. For a given "bare" disorder strength $\varkappa_0$, the renormalized dimensionless disorder strength γ and the characteristic energy Ω of the long-wave behavior of disorder-averaged observables are related by the RG equation (see Appendix for a detailed derivation)

$$\frac{\partial \gamma}{\partial \ln \Omega} = -\varepsilon\gamma - \gamma^2 - \frac{1}{2}\gamma^3 + \dots . \tag{8}$$

The dependence of Ω on the frequency ω is described by the RG equation

$$\left(\frac{\partial \ln \Omega}{\partial \ln \omega} \right)^{-1} = 1 + \frac{\gamma}{2} + \frac{\gamma^2}{8} + \dots . \tag{9}$$

Our two-loop RG equations (8) and (9) are consistent with the previous studies of Weyl fermions in $d = 2 - \varepsilon$ dimensions: in the framework of Gross-Neveu model in Refs. [22–27] and of graphene in Ref. [21].

Equation (8) shows that the dimensionless disorder strength grows or decreases depending on whether or not it exceeds a critical disorder strength

$$\gamma_c = -\varepsilon - \frac{\varepsilon^2}{2} + \dots . \tag{10}$$

The existence of such a repulsive fixed point signals a transition, discussed in the literature [1–5,10,11,17,19,20,33,34], between a weak-disorder phase and a strong-disorder phase.

Using that near the transition $\frac{\partial \ln(\gamma - \gamma_c)}{\partial \ln \Omega} = -\nu^{-1}$ and Eq. (8) holds, we obtain the correlation-length critical exponent (1). The divergence of ν in the $\varepsilon \to 0$ limit reflects the fact that $d = 2$ ($\varepsilon = 0$) is the lower critical dimension for this transition.

Our analysis predicts $\omega \propto \Omega^z$ at the critical disorder strength $\gamma = \gamma_c$. Equation (9) then gives the dynamical critical exponent (2).

We note that for small $\varepsilon \ll 1$ the correlation-length exponent ν, Eq. (1), satisfies Harris criterion (Chayes inequality) [35,36] $\nu \geqslant 2/d$. Because the correlation length $\xi \propto \Omega^{-1} \propto \omega^{-\frac{1}{z}}$ can be measured as a function of the energy ω for $\varkappa = \varkappa_c$ as well as a function of disorder strength $\xi \propto |\varkappa - \varkappa_c|^{-\nu}$ for $\omega = 0$, a similar criterion can be applied heuristically to the exponent $\tilde{\nu} = 1/z$, yielding $z \leqslant d/2$, consistent with our result (2).

In conclusion, we have presented a two-loop renormalization-group analysis of the critical properties of the unconventional disorder-driven transition for Weyl fermions above two dimensions and found the correlation-length and dynamical critical exponents, Eqs. (1) and (2). The beta

functions that we obtain are consistent with those for graphene and Gross-Neveu models studied previously in the literature[2].

Note added. After posting this paper on arXiv, the results of Refs. [11,20], contradicting our conclusions here, have been withdrawn by their authors; the claim of $z = 3/2$ being the exact dynamical exponent has been removed [37] by the authors of Ref. [20], while the results of Ref. [11] for the critical exponents have been retracted in erratum [38].

ACKNOWLEDGMENTS

We appreciate useful discussions with A.W.W. Ludwig. Our work was supported by the Alexander von Humboldt Foundation through the Feodor Lynen Research Fellowship (S.V.S.) and by the NSF grants DMR-1001240 (L.R. and S.V.S.), DMR-1205303(V.G. and S.V.S.), PHY-1211914 (V.G. and S.V.S.), and PHY-1125844 (S.V.S.). L.R. also acknowledges support by the Simons Investigator award from the Simons Foundation.

APPENDIX A: RENORMALIZATION SCHEME

Disorder-averaged observables, e.g., the density of states or conductivity, calculated perturbatively in disorder strength using action (4) in dimensions $d > 2$ contain ultravioletly divergent contributions that require an appropriate renormalization-group treatment.

In this paper, we use the minimal-subtraction renormalization-group scheme [32]. The respective integrals in this scheme are evaluated in lower $d = 2 - \varepsilon$ dimensions ($\varepsilon > 0$), to ensure their ultraviolet convergence, making analytic continuation to higher dimensions ($\varepsilon < 0$) in the end of the calculation. Also, as we show below, the infrared convergence of momentum integrals is ensured by using Matsubara frequencies $i\Omega$ in place of real frequencies. The renormalization procedure consists in calculating perturbative corrections to the disorder-free particle propagator

$$G(i\Omega,\mathbf{p}) = (i\Omega - \hat{\boldsymbol{\sigma}}\mathbf{p})^{-1} = -\frac{i\Omega + \hat{\boldsymbol{\sigma}}\mathbf{p}}{\Omega^2 + p^2} \tag{A1}$$

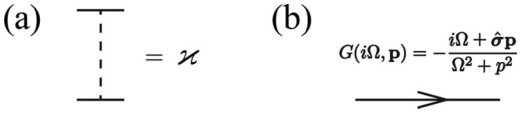

FIG. 1. Elements of the diagrammatic technique: (a) impurity line and (b) propagator.

and the coupling $\varkappa$ in the Lagrangian (6) and adding counterterms $\mathcal{L}_{\text{counter}}$ to the Lagrangian in order to cancel divergent (in powers of $1/\varepsilon$) contributions. The renormalized quantities $\varkappa$ and Ω can then be related to the "bare" $\varkappa_0$ and ω by comparing the initial Lagrangian (4) and the Lagrangian (5) expressed in the renormalized variables.

Perturbative corrections to the propagator and disorder strength can be obtained straightforwardly using the Lagrangian (6). For convenience we utilize the conventional disorder-averaging diagrammatic technique [39], Fig. 1. The impurity line, Fig 1(a), is a tensor product of two operators $\hat{\tau}_1 \otimes \hat{\tau}_2$ in the pseudospin subspaces that correspond to the two ends of the impurity line. Hereinafter, scalar expressions for impurity lines are implied to be multiplied by $\mathbb{1} \otimes \mathbb{1}$.

1. Integrals in $d = 2 - \varepsilon$ dimensions

When evaluating diagrams below, we use the following values of momentum integrals in dimension $2 - \varepsilon$:

$$\int_{\mathbf{p}} \frac{1}{p^2 + \Omega^2} = \frac{C_{2-\varepsilon}}{\varepsilon}\Omega^{-\varepsilon} + \mathcal{O}(\varepsilon), \tag{A2a}$$

$$\int_{\mathbf{p}} \frac{1}{(p^2 + \Omega^2)^2} = \frac{1}{2}C_{2-\varepsilon}\Omega^{-2-\varepsilon} + \mathcal{O}(\varepsilon), \tag{A2b}$$

$$\int_{\mathbf{p}} \frac{1}{(p^2 + \Omega^2)^3} = \frac{1}{4}C_{2-\varepsilon}\Omega^{-4-\varepsilon} + \mathcal{O}(\varepsilon), \tag{A2c}$$

$$\int_{\mathbf{p}} \frac{1}{(i\Omega - \hat{\boldsymbol{\sigma}}\mathbf{p})^2} = \left(\frac{1}{\varepsilon} - 1\right)C_{2-\varepsilon}\Omega^{-\varepsilon} + \mathcal{O}(\varepsilon), \tag{A2d}$$

$$\int_{\mathbf{p}} \frac{1}{(i\Omega - \hat{\boldsymbol{\sigma}}\mathbf{p})^3} = -\frac{iC_{2-\varepsilon}}{2}\Omega^{-1-\varepsilon} + \mathcal{O}(\varepsilon), \tag{A2e}$$

$$\int_{\mathbf{p},\mathbf{q}} \frac{1}{(\Omega^2 + p^2)(\Omega^2 + q^2)[\Omega^2 + (\mathbf{p}+\mathbf{q})^2]} = \mathcal{O}(1), \tag{A3a}$$

$$\int_{\mathbf{p},\mathbf{q}} \frac{\mathbf{pq}}{(\Omega^2 + p^2)(\Omega^2 + q^2)[\Omega^2 + (\mathbf{p}+\mathbf{q})^2]} = -\frac{1}{2}\left(\frac{C_{2-\varepsilon}}{\varepsilon}\Omega^{-\varepsilon}\right)^2 + \mathcal{O}(1), \tag{A3b}$$

$$\int_{\mathbf{p},\mathbf{q}} \frac{(\mathbf{p}\hat{\boldsymbol{\sigma}})(\mathbf{q}\hat{\boldsymbol{\sigma}})}{(\Omega^2 + p^2)(\Omega^2 + q^2)[\Omega^2 + (\mathbf{p}+\mathbf{q})^2]} = -\frac{1}{2}\left(\frac{C_{2-\varepsilon}}{\varepsilon}\Omega^{-\varepsilon}\right)^2 + \mathcal{O}(1), \tag{A3c}$$

$$\int_{\mathbf{p},\mathbf{q}} \frac{(\mathbf{p}\hat{\boldsymbol{\sigma}})(\mathbf{q}\hat{\boldsymbol{\sigma}})}{(\Omega^2 + p^2)^2[\Omega^2 + (\mathbf{p}+\mathbf{q})^2]} = -\left(\frac{C_{2-\varepsilon}}{\varepsilon}\Omega^{-\varepsilon}\right)^2\left(1 - \frac{\varepsilon}{2}\right) + \mathcal{O}(1), \tag{A3d}$$

[2]We note that the sign of the coupling γ in the disordered problem under consideration is opposite to that of the respective models studied in high-energy literature for repulsively interacting fermions, which reflects in different signs of even-in-γ terms of beta functions.

$$\int_{\mathbf{p},\mathbf{q}} \frac{(\hat{\boldsymbol{\sigma}}\mathbf{p})(\hat{\boldsymbol{\sigma}}\mathbf{q})}{(\Omega^2+p^2)^2(\Omega^2+q^2)[\Omega^2+(\mathbf{p}+\mathbf{q})^2]} = \mathcal{O}(1), \tag{A3e}$$

$$\int_{\mathbf{p},\mathbf{q}} \frac{\mathbf{pq}}{(\Omega^2+p^2)^2(\Omega^2+q^2)[\Omega^2+(\mathbf{p}+\mathbf{q})^2]} = \mathcal{O}(1), \tag{A3f}$$

where the coefficient $C_{2-\varepsilon} = 2(4\pi)^{\frac{\varepsilon}{2}-1}/\,\Gamma(1-\frac{\varepsilon}{2})$ is defined after Eq. (7), and $\int_{\mathbf{p}} \ldots ... = \int d\mathbf{p}/(2\pi)^d \ldots$.

Detailed calculations of integrals (A2a)–(A2c) are presented, e.g., in Ref. [32]. Integrals (A2d) and (A2e) can be reduced to similar integrals using $(i\Omega - \hat{\boldsymbol{\sigma}}\mathbf{p})^{-1} = -(i\Omega + \hat{\boldsymbol{\sigma}}\mathbf{p})/(\Omega^2+p^2)$.

Integral (A3a) can be evaluated by introducing two Feynman parametrizations [32]:

$$\begin{aligned}
&\int_{\mathbf{p},\mathbf{q}} \frac{1}{(\Omega^2+p^2)(\Omega^2+q^2)[\Omega^2+(\mathbf{p}+\mathbf{q})^2]} \\
&= \int_{\mathbf{q}} \frac{1}{\Omega^2+q^2} \int_0^1 du \int_{\mathbf{p}} \frac{1}{[\Omega^2+(1-u)p^2+u(\mathbf{p}+\mathbf{q})^2]^2} \\
&= \int_{\mathbf{q}} \frac{1}{\Omega^2+q^2} \int_0^1 du \frac{C_d \Gamma\left(2-\frac{d}{2}\right)\Gamma\left(\frac{d}{2}\right)}{2\Gamma(2)} [\Omega^2+u(1-u)q^2]^{\frac{d}{2}-2} \overset{\varepsilon\ll 1}{\approx} \frac{C_{2-\varepsilon}}{2} \int_0^1 du \int_{\mathbf{q}} \frac{1}{(\Omega^2+q^2)[\Omega^2+q^2u(1-u)]^{2-\frac{d}{2}}} \\
&\approx \left(\frac{C_{2-\varepsilon}}{2}\right)^2 \iint_0^1 du\, dt \int_{\mathbf{q}} \frac{t^{1-\frac{d}{2}}}{[\Omega^2+q^2tu(1-u)+(1-t)q^2]^{3-\frac{d}{2}}} \approx \left(\frac{C_{2-\varepsilon}}{2}\right)^2 \Omega^{2-2\varepsilon} \iint_0^1 dt\, du \frac{t^{1-\frac{d}{2}}}{[tu(1-u)+1-t]^{\frac{d}{2}}} = \mathcal{O}(1).
\end{aligned} \tag{A4}$$

Integral (A3b) can be reduced to the previous integrals by using that $\mathbf{pq} = \frac{1}{2}(\mathbf{p}+\mathbf{q})^2 - \frac{1}{2}p^2 - \frac{1}{2}q^2$.

In order to evaluate integrals (A3c)–(A3f), we note that they are invariant under the interchange of $\mathbf{p}$ and $\mathbf{q}$. They can thus be reduced to the previous integrals by replacing $(\mathbf{p}\hat{\boldsymbol{\sigma}})(\mathbf{q}\hat{\boldsymbol{\sigma}}) \to \frac{1}{2}[(\mathbf{p}\hat{\boldsymbol{\sigma}})(\mathbf{q}\hat{\boldsymbol{\sigma}}) + (\mathbf{q}\hat{\boldsymbol{\sigma}})(\mathbf{p}\hat{\boldsymbol{\sigma}})] = \frac{1}{2}(\mathbf{p}+\mathbf{q})^2 - \frac{1}{2}p^2 - \frac{1}{2}q^2$ or $\mathbf{pq} \to \frac{1}{2}(\mathbf{p}+\mathbf{q})^2 - \frac{1}{2}p^2 - \frac{1}{2}q^2$.

APPENDIX B: ONE-LOOP RENORMALIZATIONS

One-loop renormalization is mimicked by the diagrams in Fig. 2. In what follows, expressions in square brackets is our convention for the values of the respective diagrams.

Diagram 2(a), the leading-order-in-$\varkappa$ self-energy of the particles, is independent of the incoming and outgoing momenta and can be evaluated as

$$[2a] = \varkappa \int_{\mathbf{p}} (i\Omega - \hat{\boldsymbol{\sigma}}\mathbf{p})^{-1} \overset{(A2a)}{=} -i\Omega\varkappa \frac{C_{2-\varepsilon}}{\varepsilon} + \mathcal{O}(\varepsilon). \tag{B1}$$

Diagrams 2(b)–2(e) mimic the corrections to the disorder strength $\varkappa$. Because we study the long-wavelength behavior of the system (at finite frequency), these diagrams can be evaluated for zero incoming and outgoing momenta, integrating with respect to the intermediate momenta:

$$\begin{aligned}
[2b] = [2c] &= \varkappa^2 \int_{\mathbf{p}} (i\Omega - \hat{\boldsymbol{\sigma}}\mathbf{p})^{-2} \overset{(A2d)}{=} \varkappa^2 \frac{C_{2-\varepsilon}}{\varepsilon} \Omega^{-\varepsilon} + \mathcal{O}(1), \qquad \text{(B2)} \\
[2d] + [2e] &= \varkappa^2 \int_{\mathbf{p}} \frac{1}{i\Omega - \hat{\boldsymbol{\sigma}}\mathbf{p}} \otimes \frac{1}{i\Omega - \hat{\boldsymbol{\sigma}}\mathbf{p}} + \varkappa^2 \int_{\mathbf{p}} \frac{1}{i\Omega - \hat{\boldsymbol{\sigma}}\mathbf{p}} \otimes \frac{1}{i\Omega + \hat{\boldsymbol{\sigma}}\mathbf{p}} \\
&= -\varkappa^2 \int_{\mathbf{p}} \frac{2\Omega^2}{(\Omega^2+p^2)^2} = \mathcal{O}(1). \qquad \text{(B3)}
\end{aligned}$$

To cancel the divergent in $1/\varepsilon$ corrections to the scale Ω and to the disorder strength $\varkappa$, given by Eqs. (B1) and (B2),(B3), respectively, we add to the Lagrangian (6) the counterterm-Lagrangian

$$\mathcal{L}_{\text{counter}} = \int \delta^{(1)}\Omega\, \psi^\dagger\psi\, d\mathbf{r} + \frac{1}{2}\delta^{(1)}\varkappa \int (\psi^\dagger\psi)^2 d\mathbf{r}, \tag{B4}$$

$$\delta^{(1)}\varkappa = -2\varkappa^2 \frac{C_{2-\varepsilon}}{\varepsilon}\, \Omega^{-\varepsilon}, \tag{B5}$$

$$\delta^{(1)}\Omega = -\Omega\varkappa \frac{C_{2-\varepsilon}}{\varepsilon}\, \Omega^{-\varepsilon}. \tag{B6}$$

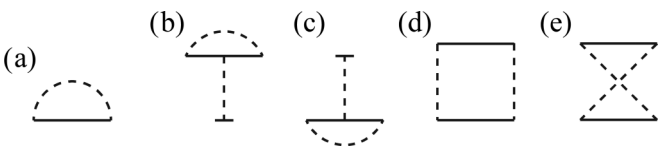

FIG. 2. Diagrams for the one-loop renormalization: (a) self-energy correction and (b)–(e) vertex corrections.

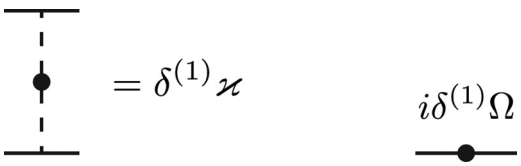

FIG. 3. Counterterms coming from the one-loop renormalisation.

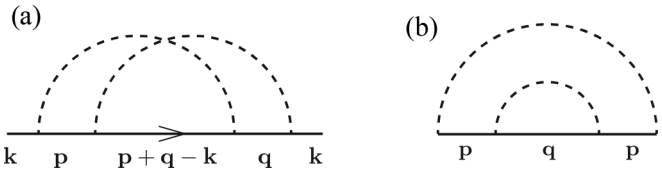

FIG. 4. Contributions to the renormalisation of the self-energy.

Equations (B5) and (B6) describe the one-loop renormalisation of the system parameters. We note that there is no one-loop renormalization of the particle velocity (the coefficient before $\hat{\boldsymbol{\sigma}}\mathbf{k}$ in the Lagrangian).

In order to take into account these one-loop corrections when performing the two-loop renormalization, we introduce additional elements to the diagrammatic technique, Fig. 3.

APPENDIX C: TWO-LOOP SELF-ENERGY RENORMALIZATION

The two-loop contribution to the particle self-energy is given by the diagrams in Figs. 4 and 5. Diagram 4(a) depends on the external momentum $\mathbf{k}$, while the other diagrams are momentum-independent. The momentum dependency of the two-loop self-energy leads to the renormalization of the particle velocity, in addition to the energy scale Ω.

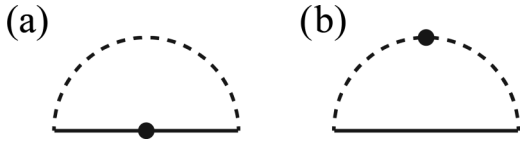

FIG. 5. Two-loop contributions to the self-energy that come from one-loop counterterms, see Fig. 3.

1. Frequency renormalization

In order to obtain the two-loop corrections to Ω, it is sufficient to evaluate the diagrams in Figs. 4 and 5 for zero external momenta.

Diagrams 4(a) and 4(b) for $\mathbf{k}=0$ are given by (in units $\varkappa^2$)

$$[4a] = -\int_{\mathbf{p},\mathbf{q}} \frac{(i\Omega+\hat{\boldsymbol{\sigma}}\mathbf{p})[i\Omega+\hat{\boldsymbol{\sigma}}(\mathbf{p}+\mathbf{q})](i\Omega+\hat{\boldsymbol{\sigma}}\mathbf{q})}{(\Omega^2+p^2)[\Omega^2+(\mathbf{p}+\mathbf{q})^2](\Omega^2+q^2)}$$

$$\overset{\text{(A3a)}}{=} -i\Omega\int_{\mathbf{p},\mathbf{q}} \frac{(\mathbf{p}\hat{\boldsymbol{\sigma}})(\mathbf{q}\hat{\boldsymbol{\sigma}})+(\mathbf{p}\hat{\boldsymbol{\sigma}})(\mathbf{p}\hat{\boldsymbol{\sigma}}+\mathbf{q}\hat{\boldsymbol{\sigma}})+(\mathbf{p}\hat{\boldsymbol{\sigma}}+\mathbf{q}\hat{\boldsymbol{\sigma}})(\mathbf{q}\hat{\boldsymbol{\sigma}})}{(\Omega^2+p^2)(\Omega^2+q^2)[\Omega^2+(\mathbf{p}+\mathbf{q})^2]} + \mathcal{O}(1) \overset{\text{(A3c)}}{=} -\frac{i\Omega}{2}\left(\frac{C_{2-\varepsilon}}{\varepsilon}\Omega^{-\varepsilon}\right)^2 + \mathcal{O}(1), \tag{C1}$$

$$[4b] \overset{\text{(A2a),(A2d)}}{=} -i\Omega\left(\frac{C_{2-\varepsilon}}{\varepsilon}\Omega^{-\varepsilon}\right)^2(1-\varepsilon)+\mathcal{O}(1). \tag{C2}$$

Diagrams of the second order in the disorder strength $\varkappa$ that contain the one-loop counterterms, see Fig. 3, are shown in Fig. 5.

$$[5a] = \varkappa\,\delta^{(1)}\varkappa\int_{\mathbf{p}}(i\Omega-\hat{\boldsymbol{\sigma}}\mathbf{p})^{-2} \overset{\text{(A2d),(B5)}}{=} i\Omega\varkappa^2\left(\frac{C_{2-\varepsilon}}{\varepsilon}\Omega^{-\varepsilon}\right)^2(1-\varepsilon)+\mathcal{O}(1), \tag{C3}$$

$$[5b] = 2i\Omega\varkappa^2\left(\frac{C_{2-\varepsilon}}{\varepsilon}\Omega^{-\varepsilon}\right)^2+\mathcal{O}(1). \tag{C4}$$

2. Velocity renormalization

The velocity renormalization is determined by the linear-in-$\mathbf{k}$ contribution to the self-energy. In order to obtain it, we expand to the linear order the $\mathbf{k}$-dependent propagator in diagram 4(a):

$$G_0(i\Omega,\mathbf{p}+\mathbf{q}-\mathbf{k}) \approx G_0(i\Omega,\mathbf{p}+\mathbf{q}) - G_0(i\Omega,\mathbf{p}+\mathbf{q})(\hat{\boldsymbol{\sigma}}\mathbf{k})G_0(i\Omega,\mathbf{p}+\mathbf{q}). \tag{C5}$$

The diagram, corresponding to the linear-in-$\mathbf{k}$ contribution, is shown in Fig. 6. In units $\varkappa^2$

$$[6] = -\int_{\mathbf{p},\mathbf{q}} \frac{1}{i\Omega-\hat{\boldsymbol{\sigma}}\mathbf{p}}\frac{1}{i\Omega-\hat{\boldsymbol{\sigma}}(\mathbf{p}+\mathbf{q})}\hat{\boldsymbol{\sigma}}\mathbf{k}\frac{1}{i\Omega-\hat{\boldsymbol{\sigma}}(\mathbf{p}+\mathbf{q})}\frac{1}{i\Omega-\hat{\boldsymbol{\sigma}}\mathbf{q}}$$

$$= -\int_{\mathbf{p},\mathbf{q}} \frac{(i\Omega+\hat{\boldsymbol{\sigma}}\mathbf{p})[i\Omega+\hat{\boldsymbol{\sigma}}(\mathbf{p}+\mathbf{q})](\hat{\boldsymbol{\sigma}}\mathbf{k})[i\Omega+\hat{\boldsymbol{\sigma}}(\mathbf{p}+\mathbf{q})](i\Omega+\hat{\boldsymbol{\sigma}}\mathbf{q})}{(\Omega^2+p^2)[\Omega^2+(\mathbf{p}+\mathbf{q})^2]^2(\Omega^2+q^2)}. \tag{C6}$$

Using that $(\hat{\boldsymbol{\sigma}}\mathbf{p}_1)(\hat{\boldsymbol{\sigma}}\mathbf{p}_2)+(\hat{\boldsymbol{\sigma}}\mathbf{p}_2)(\hat{\boldsymbol{\sigma}}\mathbf{p}_1)\equiv 2\mathbf{p}_1\mathbf{p}_2$, Eq. (C6) gives

$$[6] = \int_{\mathbf{p},\mathbf{q}} \frac{(i\Omega+\hat{\boldsymbol{\sigma}}\mathbf{p})(\hat{\boldsymbol{\sigma}}\mathbf{k})(i\Omega+\hat{\boldsymbol{\sigma}}\mathbf{q})}{(\Omega^2+p^2)[\Omega^2+(\mathbf{p}+\mathbf{q})^2](\Omega^2+q^2)} + I_1, \tag{C7}$$

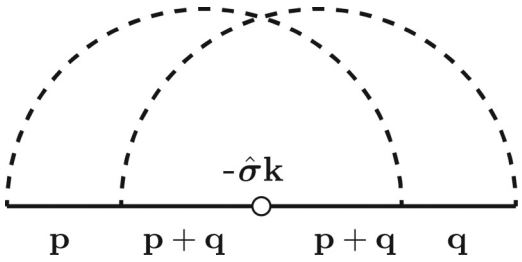

FIG. 6. Diagram for the velocity renormalization.

where

$$I_1 = -2\int_{\mathbf{p},\mathbf{q}} \frac{(i\Omega+\hat{\boldsymbol{\sigma}}\mathbf{p})[i\Omega+\hat{\boldsymbol{\sigma}}(\mathbf{p}+\mathbf{q})](i\Omega+\hat{\boldsymbol{\sigma}}\mathbf{q})}{(\Omega^2+p^2)[\Omega^2+(\mathbf{p}+\mathbf{q})^2]^2(\Omega^2+q^2)} \times(\mathbf{p}+\mathbf{q})\mathbf{k}. \tag{C8}$$

Let us demonstrate that I_1, Eq. (C8), does not contain $1/\varepsilon$ or $1/\varepsilon^2$ singularities. Replacing in the numerator $(i\Omega+\hat{\boldsymbol{\sigma}}\mathbf{p})[i\Omega+\hat{\boldsymbol{\sigma}}(\mathbf{p}+\mathbf{q})](i\Omega+\hat{\boldsymbol{\sigma}}\mathbf{q}) \to p^2(\hat{\boldsymbol{\sigma}}\mathbf{q}) + q^2(\hat{\boldsymbol{\sigma}}\mathbf{p}) - 2\Omega^2\hat{\boldsymbol{\sigma}}(\mathbf{p}+\mathbf{q})$ (as the other contributions vanish) and using (A3a) gives

$$I_1 = -2\int_{\mathbf{p},\mathbf{q}} \frac{p^2(\hat{\boldsymbol{\sigma}}\mathbf{q})+q^2(\hat{\boldsymbol{\sigma}}\mathbf{p})}{(\Omega^2+p^2)[\Omega^2+(\mathbf{p}+\mathbf{q})^2]^2(\Omega^2+q^2)}(\mathbf{p}+\mathbf{q})\mathbf{k} + \mathcal{O}(1). \tag{C9}$$

Using that the integral in (C9) is invariant with respect to interchanging $\mathbf{p}$ and $\mathbf{q}$ and to changing signs of momentum components $(p_\alpha, q_\alpha \to -p_\alpha, -q_\alpha)$, we replace $(\mathbf{q}\hat{\boldsymbol{\sigma}})\cdot[(\mathbf{p}+\mathbf{q})\mathbf{k}] \equiv \sum_{\alpha,\beta}\sigma_\alpha q_\alpha(p+q)_\beta k_\beta \to \sum_\alpha \sigma_\alpha q_\alpha (p+q)_\alpha k_\alpha \to \frac{1}{d}\mathbf{q}(\mathbf{p}+\mathbf{q})\cdot(\hat{\boldsymbol{\sigma}}\mathbf{k})$ and arrive at

$$\begin{aligned} I_1 &= -\frac{4}{d}\int_{\mathbf{p},\mathbf{q}} \frac{p^2\mathbf{q}(\mathbf{p}+\mathbf{q})}{(\Omega^2+p^2)[\Omega^2+(\mathbf{p}+\mathbf{q})^2]^2(\Omega^2+q^2)}\hat{\boldsymbol{\sigma}}\mathbf{k} \\ &= -\frac{4}{d}\int_{\mathbf{p},\mathbf{q}} \frac{\mathbf{q}(\mathbf{p}+\mathbf{q})}{(\Omega^2+q^2)[\Omega^2+(\mathbf{p}+\mathbf{q})^2]} + \frac{4}{d}\Omega^2\int_{\mathbf{p},\mathbf{q}} \frac{\mathbf{q}(\mathbf{q}+\mathbf{p})}{(\Omega^2+p^2)[\Omega^2+(\mathbf{p}+\mathbf{q})^2]^2(\Omega^2+q^2)} \overset{\text{(A3f)}}{=} \mathcal{O}(1). \end{aligned} \tag{C10}$$

Equations (C7), (C8), and (C10) give

$$\begin{aligned} [6] &= \int_{\mathbf{p},\mathbf{q}} \frac{(\hat{\boldsymbol{\sigma}}\mathbf{p})(\hat{\boldsymbol{\sigma}}\mathbf{k})(\hat{\boldsymbol{\sigma}}\mathbf{q})}{(\Omega^2+p^2)(\Omega^2+q^2)[\Omega^2+(\mathbf{p}+\mathbf{q})^2]} + \mathcal{O}(1) \\ &= \left(\frac{2}{d}-1\right)\int_{\mathbf{p},\mathbf{q}} \frac{\mathbf{pq}}{(\Omega^2+p^2)(\Omega^2+q^2)[\Omega^2+(\mathbf{p}+\mathbf{q})^2]}\hat{\boldsymbol{\sigma}}\mathbf{k} + \mathcal{O}(1) \overset{\text{(A3b)}}{=} -\frac{1}{4\varepsilon}(C_{2-\varepsilon}\Omega^{-\varepsilon})^2\hat{\boldsymbol{\sigma}}\mathbf{k} + \mathcal{O}(1). \end{aligned} \tag{C11}$$

APPENDIX D: TWO-LOOP VERTEX RENORMALISATION

The two-loop renormalization of the disorder strength $\varkappa$ corresponds to the diagrams in Figs. 7–13 (we show only topologically inequivalent diagrams). In what immediately follows we present a detailed calculation of each of these diagrams. For simplicity, all expressions for the diagrams are given in units $\varkappa^3$.

$$[7a] = \left[\int_{\mathbf{p}} \frac{1}{(i\Omega-\hat{\boldsymbol{\sigma}}\mathbf{p})^2}\right]^2 \overset{\text{(A2a)}}{=} (C_{2-\varepsilon}\Omega^{-\varepsilon})\left(\frac{1}{\varepsilon^2}-\frac{2}{\varepsilon}\right)+\mathcal{O}(1), \tag{D1}$$

$$\begin{aligned} [7b] &= \int_{\mathbf{p},\mathbf{q}} \frac{1}{i\Omega-\hat{\boldsymbol{\sigma}}\mathbf{p}}\frac{1}{[i\Omega-\hat{\boldsymbol{\sigma}}(\mathbf{p}+\mathbf{q})]^2}\frac{1}{i\Omega-\hat{\boldsymbol{\sigma}}\mathbf{q}} = \int_{\mathbf{p},\mathbf{q}} \frac{(i\Omega+\hat{\boldsymbol{\sigma}}\mathbf{p})[i\Omega+\hat{\boldsymbol{\sigma}}(\mathbf{p}+\mathbf{q})]^2(i\Omega+\hat{\boldsymbol{\sigma}}\mathbf{q})}{(\Omega^2+p^2)[\Omega^2+(\mathbf{p}+\mathbf{q})^2]^2(\Omega^2+q^2)} \\ &= \int_{\mathbf{p},\mathbf{q}} \frac{(\hat{\boldsymbol{\sigma}}\mathbf{p})(\hat{\boldsymbol{\sigma}}\mathbf{q})(\mathbf{p}+\mathbf{q})^2}{(\Omega^2+p^2)[\Omega^2+(\mathbf{p}+\mathbf{q})^2]^2(\Omega^2+q^2)} \\ &\quad -\Omega^2\int_{\mathbf{p},\mathbf{q}} \frac{2(\hat{\boldsymbol{\sigma}}\mathbf{p})(\hat{\boldsymbol{\sigma}}\mathbf{p}+\hat{\boldsymbol{\sigma}}\mathbf{q})+2(\hat{\boldsymbol{\sigma}}\mathbf{p}+\hat{\boldsymbol{\sigma}}\mathbf{q})(\hat{\boldsymbol{\sigma}}\mathbf{q})+(\hat{\boldsymbol{\sigma}}\mathbf{p})(\hat{\boldsymbol{\sigma}}\mathbf{q})}{(\Omega^2+p^2)[\Omega^2+(\mathbf{p}+\mathbf{q})^2]^2(\Omega^2+q^2)}+\mathcal{O}(1) \\ &\overset{\text{(A3a)}}{=} \int_{\mathbf{p},\mathbf{q}} \frac{(\hat{\boldsymbol{\sigma}}\mathbf{p})(\hat{\boldsymbol{\sigma}}\mathbf{q})}{(\Omega^2+p^2)[\Omega^2+(\mathbf{p}+\mathbf{q})^2](\Omega^2+q^2)} - 2\Omega^2\int_{\mathbf{p},\mathbf{q}} \frac{(\hat{\boldsymbol{\sigma}}\mathbf{p})(\hat{\boldsymbol{\sigma}}\mathbf{q})}{(\Omega^2+p^2)[\Omega^2+(\mathbf{p}+\mathbf{q})^2]^2(\Omega^2+q^2)}+\mathcal{O}(1) \\ &= \int_{\mathbf{p},\mathbf{q}} \frac{(\hat{\boldsymbol{\sigma}}\mathbf{p})(\hat{\boldsymbol{\sigma}}\mathbf{q})}{(\Omega^2+p^2)[\Omega^2+(\mathbf{p}+\mathbf{q})^2](\Omega^2+q^2)} - \Omega^2\int_{\mathbf{p},\mathbf{q}} \frac{(\mathbf{p}+\mathbf{q})^2-p^2-q^2}{(\Omega^2+p^2)[\Omega^2+(\mathbf{p}+\mathbf{q})^2]^2(\Omega^2+q^2)}+\mathcal{O}(1) \\ &\overset{\text{(A3c),(A3b),(A2b),(A2d)}}{=} -\frac{1}{2}\varkappa^3(C_{2-\varepsilon}\Omega^{-\varepsilon})^2\left(\frac{1}{\varepsilon^2}-\frac{2}{\varepsilon}\right)+\mathcal{O}(1), \end{aligned} \tag{D2}$$

$$\begin{aligned} [7c] &= \int_{\mathbf{p},\mathbf{q}} \frac{1}{(i\Omega-\hat{\boldsymbol{\sigma}}\mathbf{p})^2}\frac{1}{i\Omega-\hat{\boldsymbol{\sigma}}(\mathbf{p}+\mathbf{q})}\frac{1}{i\Omega-\hat{\boldsymbol{\sigma}}\mathbf{q}} \\ &\overset{\mathbf{p}+\mathbf{q}\to\underline{\mathbf{p}},\mathbf{q}\to-\mathbf{q}}{=} \int_{\mathbf{p},\mathbf{q}} \frac{[i\Omega+\hat{\boldsymbol{\sigma}}(\mathbf{p}+\mathbf{q})]^2}{[\Omega^2+(\mathbf{p}+\mathbf{q})^2]}\frac{i\Omega+\hat{\boldsymbol{\sigma}}\mathbf{p}}{\Omega^2+p^2}\frac{i\Omega-\hat{\boldsymbol{\sigma}}\mathbf{q}}{\Omega^2+q^2} \end{aligned}$$

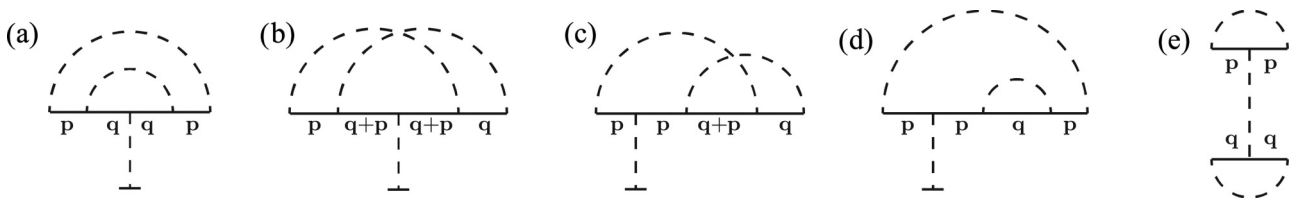

FIG. 7. Contributions to the two-loop renormalization of the impurity line.

$$= -\int_{\mathbf{p},\mathbf{q}} \frac{(\mathbf{p}+\mathbf{q})^2(\hat{\boldsymbol{\sigma}}\mathbf{p})(\hat{\boldsymbol{\sigma}}\mathbf{q})}{(\Omega^2+p^2)[\Omega^2+(\mathbf{p}+\mathbf{q})^2]^2(\Omega^2+q^2)}$$

$$-\Omega^2\int_{\mathbf{p},\mathbf{q}} \frac{2(\hat{\boldsymbol{\sigma}}\mathbf{p}+\hat{\boldsymbol{\sigma}}\mathbf{q})(\hat{\boldsymbol{\sigma}}\mathbf{p})+2(\hat{\boldsymbol{\sigma}}\mathbf{p}+\hat{\boldsymbol{\sigma}}\mathbf{q})(\hat{\boldsymbol{\sigma}}\mathbf{q})-(\hat{\boldsymbol{\sigma}}\mathbf{p})(\hat{\boldsymbol{\sigma}}\mathbf{q})}{(\Omega^2+p^2)[\Omega^2+(\mathbf{p}+\mathbf{q})^2]^2(\Omega^2+q^2)} + \mathcal{O}(1)$$

$$= -[7b] + \mathcal{O}(1) = \frac{1}{2}\varkappa^3(C_{2-\varepsilon}\Omega^{-\varepsilon})^2\left(\frac{1}{\varepsilon^2}-\frac{2}{\varepsilon}\right)+\mathcal{O}(1), \tag{D3}$$

$$[7\mathrm{d}] = \int_{\mathbf{p}}\left(\frac{1}{i\Omega-\hat{\boldsymbol{\sigma}}\mathbf{p}}\right)^3\int_{\mathbf{q}}\frac{1}{i\Omega-\hat{\boldsymbol{\sigma}}\mathbf{p}} \overset{\text{(A2a),(A2e)}}{=} -\frac{1}{2\varepsilon}(C_{2-\varepsilon}\Omega^{-\varepsilon})^2+\mathcal{O}(1), \tag{D4}$$

$$[7\mathrm{e}] = \int_{\mathbf{p}}\frac{1}{(i\Omega-\hat{\boldsymbol{\sigma}}\mathbf{p})^2}\otimes\int_{\mathbf{q}}\frac{1}{(i\Omega-\hat{\boldsymbol{\sigma}}\mathbf{q})^2} \overset{\text{(A2d)}}{=} (C_{2-\varepsilon}\Omega^{-\varepsilon})^2\left(\frac{1}{\varepsilon^2}-\frac{2}{\varepsilon}\right)+\mathcal{O}(1). \tag{D5}$$

$$[8] = \int_{\mathbf{p},\mathbf{q}}\frac{1}{i\Omega-\hat{\boldsymbol{\sigma}}\mathbf{p}}\frac{1}{i\Omega-\hat{\boldsymbol{\sigma}}(\mathbf{p}+\mathbf{q})}\frac{1}{i\Omega-\hat{\boldsymbol{\sigma}}\mathbf{q}}\otimes\left(\frac{1}{i\Omega-\hat{\boldsymbol{\sigma}}\mathbf{q}}+\frac{1}{i\Omega+\hat{\boldsymbol{\sigma}}\mathbf{q}}\right)$$

$$= 2i\Omega\int\frac{(i\Omega+\hat{\boldsymbol{\sigma}}\mathbf{p})[i\Omega+\hat{\boldsymbol{\sigma}}(\mathbf{p}+\mathbf{q})](i\Omega+\hat{\boldsymbol{\sigma}}\mathbf{q})}{(\Omega^2+p^2)[\Omega^2+(\mathbf{p}+\mathbf{q})^2](\Omega^2+q^2)^2}$$

$$= -2\Omega^2\int_{\mathbf{p},\mathbf{q}}\frac{(\hat{\boldsymbol{\sigma}}\mathbf{p})(\hat{\boldsymbol{\sigma}}\mathbf{q})+(\mathbf{p}+\mathbf{q})^2}{(\Omega^2+p^2)[\Omega^2+(\mathbf{p}+\mathbf{q})^2](\Omega^2+q^2)^2}+\mathcal{O}(1)$$

$$= -\Omega^2\int_{\mathbf{p},\mathbf{q}}\frac{3(\mathbf{p}+\mathbf{q})^2-p^2-q^2}{(\Omega^2+p^2)[\Omega^2+(\mathbf{p}+\mathbf{q})^2](\Omega^2+q^2)^2}$$

$$= -3\Omega^2\int_{\mathbf{p},\mathbf{q}}\frac{1}{(\Omega^2+p^2)(\Omega^2+q^2)^2}+\Omega^2\int_{\mathbf{p},\mathbf{q}}\frac{1}{[\Omega^2+(\mathbf{q}+\mathbf{p})^2](\Omega^2+q^2)^2}+\mathcal{O}(1)$$

$$\overset{\text{(A2a),(A2b)}}{=} -\frac{1}{\varepsilon}(C_{2-\varepsilon}\Omega^{-\varepsilon})^2+\mathcal{O}(1), \tag{D6}$$

$$[9] = \int_{\mathbf{p},\mathbf{q}}\frac{1}{i\Omega-\hat{\boldsymbol{\sigma}}\mathbf{p}}\frac{1}{i\Omega-\hat{\boldsymbol{\sigma}}(\mathbf{p}+\mathbf{q})}\frac{1}{i\Omega-\hat{\boldsymbol{\sigma}}\mathbf{p}}\otimes\left(\frac{1}{i\Omega-\hat{\boldsymbol{\sigma}}\mathbf{q}}+\frac{1}{i\Omega+\hat{\boldsymbol{\sigma}}\mathbf{q}}\right)$$

$$= 2i\Omega\int\frac{(i\Omega+\hat{\boldsymbol{\sigma}}\mathbf{p})[i\Omega+\hat{\boldsymbol{\sigma}}(\mathbf{p}+\mathbf{q})](i\Omega+\hat{\boldsymbol{\sigma}}\mathbf{p})}{(\Omega^2+p^2)^2[\Omega^2+(\mathbf{p}+\mathbf{q})^2](\Omega^2+q^2)} = -2\Omega^2\int_{\mathbf{p},\mathbf{q}}\frac{(\mathbf{p}^2+\mathbf{q}^2)-p^2-q^2}{(\Omega^2+p^2)^2[\Omega^2+(\mathbf{p}+\mathbf{q})^2](\Omega^2+q^2)}+\mathcal{O}(1)$$

$$\overset{\text{(A3a)}}{=} -2\Omega^2\int_{\mathbf{p},\mathbf{q}}\frac{1}{(\Omega^2+p^2)^2(\Omega^2+q^2)}+2\Omega^2\int_{\mathbf{p},\mathbf{q}}\frac{1}{(\Omega^2+p^2)^2[\Omega^2+(\mathbf{p}+\mathbf{q})^2]}+\mathcal{O}(1)=\mathcal{O}(1), \tag{D7}$$

$$[10] = \int_{\mathbf{p},\mathbf{q}}\frac{1}{i\Omega-\hat{\boldsymbol{\sigma}}\mathbf{p}}\frac{1}{i\Omega-\hat{\boldsymbol{\sigma}}\mathbf{q}}\frac{1}{i\Omega-\hat{\boldsymbol{\sigma}}\mathbf{p}}\otimes\left(\frac{1}{i\Omega-\hat{\boldsymbol{\sigma}}\mathbf{p}}+\frac{1}{i\Omega+\hat{\boldsymbol{\sigma}}\mathbf{p}}\right)$$

$$\overset{\text{(A2a)}}{=} \left[-i\Omega\frac{C_{2-\varepsilon}}{\varepsilon}\Omega^{-\varepsilon}+\mathcal{O}(\varepsilon)\right]\cdot 2i\Omega\int_{\mathbf{p}}\frac{(2i\Omega+\hat{\boldsymbol{\sigma}}\mathbf{p})^2}{(\Omega^2+p^2)^3}$$

$$= 2\Omega^2\left[\frac{C_{2-\varepsilon}}{\varepsilon}+\mathcal{O}(\varepsilon)\right]\cdot\left[\int_{\mathbf{p}}\frac{1}{(\Omega^2+p^2)^2}-2\Omega^2\int_{\mathbf{p}}\frac{1}{(\Omega^2+p^2)^3}\right]$$

$$\overset{\text{(A2b),(A2b)}}{=} \frac{1}{\varepsilon}\cdot\mathcal{O}(\varepsilon)=\mathcal{O}(1). \tag{D8}$$

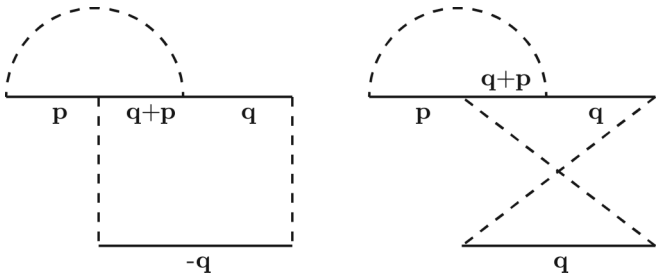

FIG. 8. Contribution to the two-loop renormalization of the impurity line.

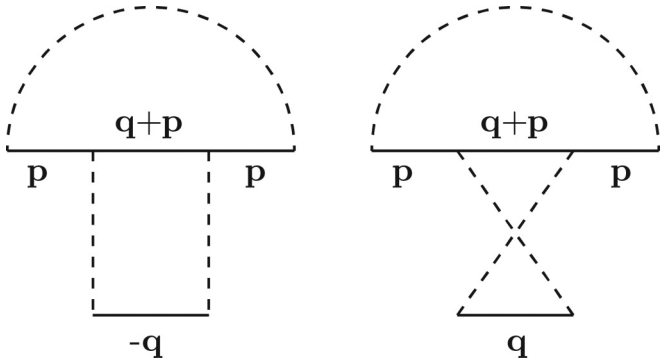

FIG. 9. Contribution to the two-loop renormalization of the impurity line.

The sum of the two diagrams in Fig. 11 is given by

$$[11] = \int_{\mathbf{p},\mathbf{q}} \frac{1}{i\Omega - \hat{\boldsymbol{\sigma}}\mathbf{p}} \frac{1}{i\Omega - \hat{\boldsymbol{\sigma}}\mathbf{q}} \otimes \frac{1}{i\Omega + \hat{\boldsymbol{\sigma}}\mathbf{p}} \frac{1}{i\Omega + \hat{\boldsymbol{\sigma}}\mathbf{q}} + \int_{\mathbf{p},\mathbf{q}} \frac{1}{i\Omega - \hat{\boldsymbol{\sigma}}\mathbf{p}} \frac{1}{i\Omega - \hat{\boldsymbol{\sigma}}\mathbf{q}} \otimes \frac{1}{i\Omega - \hat{\boldsymbol{\sigma}}\mathbf{q}} \frac{1}{i\Omega - \hat{\boldsymbol{\sigma}}\mathbf{p}}$$
$$= \int_{\mathbf{p},\mathbf{q}} \frac{(i\Omega + \hat{\boldsymbol{\sigma}}\mathbf{p})(i\Omega + \hat{\boldsymbol{\sigma}}\mathbf{q}) \otimes [-2\Omega^2 + (\hat{\boldsymbol{\sigma}}\mathbf{p})(\hat{\boldsymbol{\sigma}}\mathbf{q}) + (\hat{\boldsymbol{\sigma}}\mathbf{q})(\hat{\boldsymbol{\sigma}}\mathbf{p})]}{(\Omega^2 + p^2)^2(\Omega^2 + q^2)^2}$$
$$= 2\int_{\mathbf{p},\mathbf{q}} \frac{[-\Omega^2 + (\hat{\boldsymbol{\sigma}}\mathbf{p})(\hat{\boldsymbol{\sigma}}\mathbf{q})] \otimes (-\Omega^2 + \mathbf{pq})}{(\Omega^2 + p^2)^2(\Omega^2 + q^2)^2} = 2\int_{\mathbf{p},\mathbf{q}} \frac{(\hat{\boldsymbol{\sigma}}\mathbf{p})(\hat{\boldsymbol{\sigma}}\mathbf{q}) \otimes \mathbf{pq}}{(\Omega^2 + p^2)^2(\Omega^2 + q^2)^2} + \mathcal{O}(1). \tag{D9}$$

Using that in the tensor product $(\hat{\boldsymbol{\sigma}}\mathbf{p})(\hat{\boldsymbol{\sigma}}\mathbf{q}) \otimes \mathbf{pq} = \sum_{\alpha,\beta,\gamma} \sigma_\alpha p_\alpha \sigma_\beta q_\beta \otimes p_\gamma q_\gamma$ only the terms with $\alpha = \beta = \gamma$ contribute to the integral (D9), we replace $(\hat{\boldsymbol{\sigma}}\mathbf{p})(\hat{\boldsymbol{\sigma}}\mathbf{q}) \otimes \mathbf{pq} \to \sum_\alpha p_\alpha^2 q_\alpha^2 \to \frac{1}{d} p^2 q^2$:

$$[11] = \frac{2}{d}\left[\int_{\mathbf{p}} \frac{p^2}{(\Omega^2 + p^2)^2}\right]^2 = \frac{2}{d}\left[\int_{\mathbf{p}} \frac{1}{\Omega^2 + p^2} - \Omega^2 \int_{\mathbf{p}} \frac{1}{(\Omega^2 + p^2)^2}\right]^2$$
$$= \frac{2}{2-\varepsilon}\left[\frac{1}{\varepsilon} C_{2-\varepsilon}\Omega^{-\varepsilon} - \frac{1}{2} C_{2-\varepsilon}\Omega^{-\varepsilon} + \mathcal{O}(\varepsilon)\right]^2 = \left(\frac{1}{\varepsilon^2} - \frac{1}{2\varepsilon}\right)(C_{2-\varepsilon}\Omega^{-\varepsilon})^2 + \mathcal{O}(1). \tag{D10}$$

$$[12] = \int_{\mathbf{p},\mathbf{q}} \frac{1}{i\Omega - \hat{\boldsymbol{\sigma}}\mathbf{p}} \frac{1}{i\Omega - \hat{\boldsymbol{\sigma}}\mathbf{q}} \otimes \frac{1}{i\Omega + \hat{\boldsymbol{\sigma}}\mathbf{p}} \frac{1}{i\Omega + \hat{\boldsymbol{\sigma}}(\mathbf{p}-\mathbf{q})} + \int_{\mathbf{p},\mathbf{q}} \frac{1}{i\Omega - \hat{\boldsymbol{\sigma}}\mathbf{p}} \frac{1}{i\Omega - \hat{\boldsymbol{\sigma}}\mathbf{q}} \otimes \frac{1}{i\Omega - \hat{\boldsymbol{\sigma}}(\mathbf{p}-\mathbf{q})} \frac{1}{i\Omega - \hat{\boldsymbol{\sigma}}\mathbf{p}}$$
$$= \int_{\mathbf{p},\mathbf{q}} \frac{(i\Omega + \hat{\boldsymbol{\sigma}}\mathbf{p})(i\Omega + \hat{\boldsymbol{\sigma}}\mathbf{q}) \otimes [-2\Omega^2 + (\hat{\boldsymbol{\sigma}}\mathbf{p})(\hat{\boldsymbol{\sigma}}\mathbf{p} - \hat{\boldsymbol{\sigma}}\mathbf{q}) + (\hat{\boldsymbol{\sigma}}\mathbf{p} - \hat{\boldsymbol{\sigma}}\mathbf{q})(\hat{\boldsymbol{\sigma}}\mathbf{p})]}{(\Omega^2 + p^2)^2(\Omega^2 + q^2)[\Omega^2 + (\mathbf{p}-\mathbf{q})^2]}$$
$$= 2\int_{\mathbf{p},\mathbf{q}} \frac{(i\Omega + \hat{\boldsymbol{\sigma}}\mathbf{p})(i\Omega + \hat{\boldsymbol{\sigma}}\mathbf{q}) \otimes [-\Omega^2 + \mathbf{p}(\mathbf{p}-\mathbf{q})]}{(\Omega^2 + p^2)^2(\Omega^2 + q^2)[\Omega^2 + (\mathbf{p}-\mathbf{q})^2]} = 2\int_{\mathbf{p},\mathbf{q}} \frac{[-\Omega^2 + (\hat{\boldsymbol{\sigma}}\mathbf{p})(\hat{\boldsymbol{\sigma}}\mathbf{q})][-\Omega^2 + \mathbf{p}(\mathbf{p}-\mathbf{q})]}{(\Omega^2 + p^2)^2(\Omega^2 + q^2)[\Omega^2 + (\mathbf{p}-\mathbf{q})^2]}$$
$$= 2\int_{\mathbf{p},\mathbf{q}} \frac{(\hat{\boldsymbol{\sigma}}\mathbf{p})(\hat{\boldsymbol{\sigma}}\mathbf{q}) \otimes \mathbf{p}(\mathbf{p}-\mathbf{q})}{(\Omega^2 + p^2)^2(\Omega^2 + q^2)[\Omega^2 + (\mathbf{p}-\mathbf{q})^2]} - 2\Omega^2 \int_{\mathbf{p},\mathbf{q}} \frac{(\hat{\boldsymbol{\sigma}}\mathbf{p})(\hat{\boldsymbol{\sigma}}\mathbf{q}) \otimes \mathbb{1}}{(\Omega^2 + p^2)^2(\Omega^2 + q^2)[\Omega^2 + (\mathbf{p}-\mathbf{q})^2]}$$
$$-2\Omega^2 \int_{\mathbf{p},\mathbf{q}} \frac{\mathbb{1} \otimes \mathbf{p}(\mathbf{p}-\mathbf{q})}{(\Omega^2 + p^2)^2(\Omega^2 + q^2)[\Omega^2 + (\mathbf{p}-\mathbf{q})^2]} + \mathcal{O}(1)$$
$$\overset{\text{(A3e),(A3f)}}{=} \int_{\mathbf{p},\mathbf{q}} \frac{(\hat{\boldsymbol{\sigma}}\mathbf{p})(\hat{\boldsymbol{\sigma}}\mathbf{q}) \otimes [p^2 + (\mathbf{p}-\mathbf{q})^2 - q^2]}{(\Omega^2 + p^2)^2(\Omega^2 + q^2)[\Omega^2 + (\mathbf{p}-\mathbf{q})^2]} + \mathcal{O}(1)$$
$$= \int_{\mathbf{p},\mathbf{q}} \frac{(\hat{\boldsymbol{\sigma}}\mathbf{p})(\hat{\boldsymbol{\sigma}}\mathbf{q}) \otimes \mathbb{1}}{(\Omega^2 + p^2)(\Omega^2 + q^2)[\Omega^2 + (\mathbf{p}-\mathbf{q})^2]} - \int_{\mathbf{p},\mathbf{q}} \frac{(\hat{\boldsymbol{\sigma}}\mathbf{p})(\hat{\boldsymbol{\sigma}}\mathbf{q}) \otimes \mathbb{1}}{(\Omega^2 + p^2)^2[\Omega^2 + (\mathbf{p}-\mathbf{q})^2]}$$
$$- \Omega^2 \int_{\mathbf{p},\mathbf{q}} \frac{(\hat{\boldsymbol{\sigma}}\mathbf{p})(\hat{\boldsymbol{\sigma}}\mathbf{q})}{(\Omega^2 + p^2)^2(\Omega^2 + q^2)[\Omega^2 + (\mathbf{p}-\mathbf{q})^2]} + \mathcal{O}(1)$$
$$\overset{\text{(A3c),(A3d)}}{=} \frac{1}{2}\left(\frac{C_{2-\varepsilon}}{\varepsilon}\Omega^{-\varepsilon}\right)^2 - \left(\frac{C_{2-\varepsilon}}{\varepsilon}\Omega^{-\varepsilon}\right)^2\left(1 - \frac{\varepsilon}{2}\right) + \mathcal{O}(1) = -\frac{1}{2}(C_{2-\varepsilon}\Omega^{-\varepsilon})^2\left(\frac{1}{\varepsilon^2} + \frac{1}{\varepsilon}\right) + \mathcal{O}(1). \tag{D11}$$

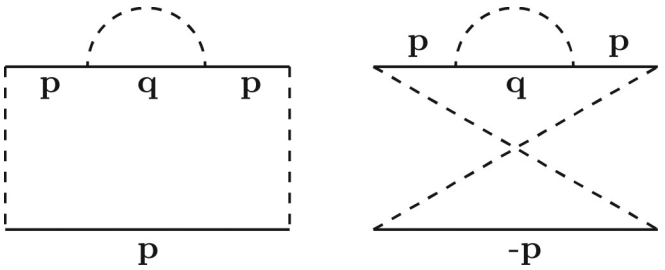

FIG. 10. Contribution to the two-loop renormalization of the impurity line.

Diagrams for the two-loop renormalization that contains the one-loop counterterms, Fig. 3, are shown in Fig. 13. Diagram 13(c) can be evaluated straightforwardly using Eq. (A2e), and the other diagrams—similarly to the corresponding one-loop diagrams in Fig. 2:

$$[13a] = [13b] = -2\varkappa^3 (C_{2-\varepsilon}\Omega^{-\varepsilon})^2 \left(\frac{1}{\varepsilon^2} - \frac{1}{\varepsilon}\right) + \mathcal{O}(1), \quad \text{(D12)}$$

$$[13c] = \frac{1}{2}\varkappa^3 (C_{2-\varepsilon}\Omega^{-\varepsilon})^2/\varepsilon + \mathcal{O}(1), \quad \text{(D13)}$$

$$[13d] = 2\varkappa^3 (C_{2-\varepsilon}\Omega^{-\varepsilon})^2/\varepsilon + \mathcal{O}(1), \quad \text{(D14)}$$

$$[13e] = \mathcal{O}(1). \quad \text{(D15)}$$

APPENDIX E: RG EQUATIONS

In the previous sections, we calculated in two loops, perturbative corrections to observable couplings Ω, $\varkappa$, and the quasiparticle velocity (coefficient before $\hat{\boldsymbol{\sigma}}\hat{\mathbf{k}}$) that come from the action (6) and contain divergent contributions $\propto 1/\varepsilon$ and $1/\varepsilon^2$. In order to cancel these divergencies, following the minimal subtraction scheme [32], we add to the action (6) the counterterm Lagrangian

$$\mathcal{L}_{\text{counter}} = -i \int \psi^\dagger [\delta(i\Omega) - \delta(\hat{\boldsymbol{\sigma}}\hat{\mathbf{k}})]\psi \, d\mathbf{r} + \frac{1}{2}\delta\varkappa \int (\psi^\dagger\psi)^2 d\mathbf{r}, \quad \text{(E1)}$$

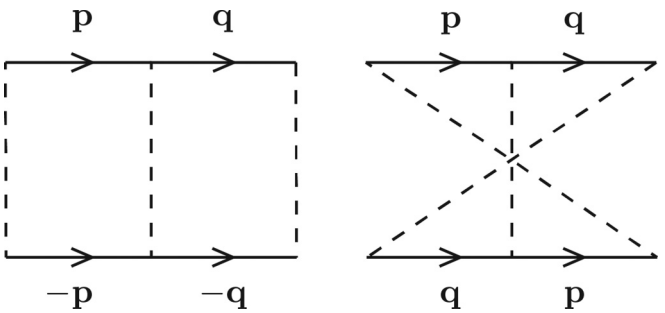

FIG. 11. Contribution to the two-loop renormalization of the impurity line.

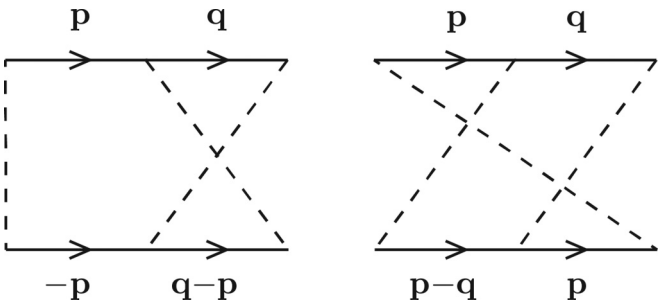

FIG. 12. Contribution to the two-loop renormalization of the impurity line.

where

$$\delta(i\Omega) = [2a] + [4a]_{\mathbf{k}=0} + [4b] + [5a] + [5b] = i\Omega\left[-\frac{1}{\varepsilon}\varkappa C_{2-\varepsilon}\Omega^{-\varepsilon} + \frac{3}{2}\frac{1}{\varepsilon^2}(\varkappa C_{2-\varepsilon}\Omega^{-\varepsilon})^2\right], \quad \text{(E2)}$$

$$\delta(\hat{\boldsymbol{\sigma}}\mathbf{k}) = -[6] = \frac{1}{4\varepsilon}(\varkappa C_{2-\varepsilon}\Omega^{-\varepsilon})^2 \hat{\boldsymbol{\sigma}}\mathbf{k}, \quad \text{(E3)}$$

$$\begin{aligned}\delta\varkappa &= -[2b-e] - 2\times[7a] - 2\times[7b] - 4\times[7c] \\ &\quad - 4\times[7d] - [7e] - 4\times[8] - 2\times[9] - 2\times[10] \\ &\quad - [11] - 2\times[12] - 2\times[13a] - 2\times[13b] \\ &\quad - 4\times[13c] - 2\times[13d] - 2\times[13e] \\ &= \varkappa\left[-\frac{2}{\varepsilon}\varkappa C_{2-\varepsilon}\Omega^{-\varepsilon} - \left(-\frac{4}{\varepsilon^2} + \frac{1}{2\varepsilon}\right)(\varkappa C_{2-\varepsilon}\Omega^{-\varepsilon})^2\right],\end{aligned} \quad \text{(E4)}$$

where we kept only the terms divergent at $\varepsilon \to 0$ and took into account the numbers of topologically equivalent diagrams.

Introducing dimensionless disorder strength, Eq. (7), the full Lagrangian (5) of the system can be rewritten in terms of

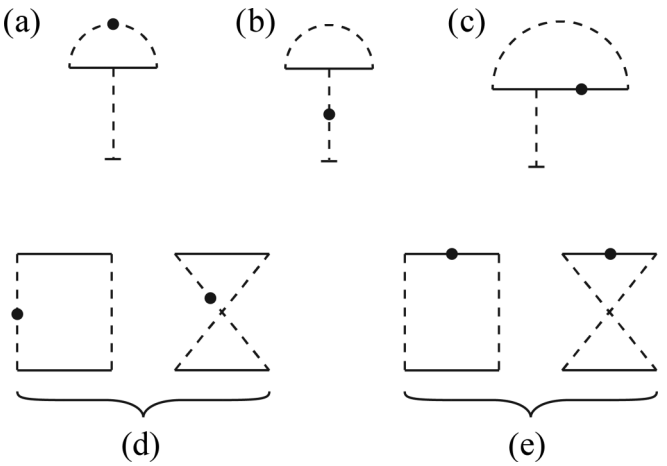

FIG. 13. Diagrams for the two-loop renormalization with one-loop counterterms.

the observable variables $\varkappa$ and Ω as

$$\mathcal{L} = -i\int \psi^\dagger\left[i\Omega\left(1-\frac{\gamma}{2\varepsilon}+\frac{3}{8}\frac{\gamma^2}{\varepsilon^2}\right)-\hat{\boldsymbol{\sigma}}\hat{\mathbf{k}}\left(1+\frac{\gamma^2}{16\varepsilon}\right)\right]\psi\, d\mathbf{r} - \frac{\gamma\Omega^\varepsilon}{4C_{2-\varepsilon}}\left(1-\frac{\gamma}{\varepsilon}-\frac{\gamma^2}{8\varepsilon}+\frac{\gamma^2}{\varepsilon^2}\right)\int(\psi^\dagger\psi)^2 d\mathbf{r}. \tag{E5}$$

The renormalized observables ψ, γ, and Ω can be related to the "bare" Φ, $\varkappa_0$, and ω by comparing the Lagrangian (E5) with the "bare" one, Eq. (4):

$$Z = 1+\frac{\gamma^2}{16\varepsilon}, \tag{E6}$$

$$\varkappa_0 = \frac{\Omega^\varepsilon}{2C_{2-\varepsilon}}\gamma\left(1-\frac{\gamma}{\varepsilon}+\frac{\gamma^2}{\varepsilon^2}-\frac{\gamma^2}{4\varepsilon}\right), \tag{E7}$$

$$\omega = \Omega\left(1-\frac{\gamma}{2\varepsilon}+\frac{3\gamma^2}{8\varepsilon^2}-\frac{\gamma^2}{16\varepsilon}\right), \tag{E8}$$

where Z describes the rescaling of the particle wave functons: $\psi = \Phi/Z^{\frac{1}{2}}$.

The energy scale Ω sets the characteristic momentum of long-wavelength behavior of the system. In order to obtain the RG flow of the renormalized disorder strength γ as a function of Ω for a given bare disorder strength $\varkappa_0$, we require

$$\frac{\partial\varkappa_0}{\partial\ln\Omega} = 0, \tag{E9}$$

which, together with Eq. (E7), gives the RG equation (8). RG equation (9) follows straightforwardly from Eq. (E8).

[1] E. Fradkin, Phys. Rev. B **33**, 3263 (1986).
[2] E. Fradkin, Phys. Rev. B **33**, 3257 (1986).
[3] K. Kobayashi, T. Ohtsuki, K.-I. Imura, and I. F. Herbut, Phys. Rev. Lett. **112**, 016402 (2014).
[4] S. V. Syzranov, L. Radzihovsky, and V. Gurarie, Phys. Rev. Lett. **114**, 166601 (2015).
[5] S. V. Syzranov, V. Gurarie, and L. Radzihovsky, Phys. Rev. B **91**, 035133 (2015).
[6] M. Gärttner, S. V. Syzranov, A. M. Rey, V. Gurarie, and L. Radzihovsky, Phys. Rev. B **92**, 041406(R) (2015).
[7] S.-M. Huang, S.-Y. Xu, I. Belopolski, C.-C. Lee, G. Chang, B. Wang, N. Alidoust, G. Bian, M. Neupane, C. Zhang *et al.*, Nature Comm. **6**, 7373 (2015).
[8] S.-Y. Xu, I. Belopolski, N. Alidoust, M. Neupane, G. Bian, C. Zhang, R. Sankar, G. Chang, Z. Yuan, C.-C. Lee *et al.*, Science **349**, 613 (2015).
[9] B. Q. Lv, H. M. Weng, B. B. Fu, X. P. Wang, H. Miao, J. Ma, P. Richard, X. C. Huang, L. X. Zhao, G. F. Chen *et al.*, Phys. Rev. X **5**, 031013 (2015).
[10] P. Goswami and S. Chakravarty, Phys. Rev. Lett. **107**, 196803 (2011).
[11] B. Roy and S. Das Sarma, Phys. Rev. B **90**, 241112(R) (2014).
[12] S. Ryu and K. Nomura, Phys. Rev. B **85**, 155138 (2012).
[13] R. Shindou and S. Murakami, Phys. Rev. B **79**, 045321 (2009).
[14] Y. Ominato and M. Koshino, Phys. Rev. B **89**, 054202 (2014).
[15] I. L. Aleiner and K. B. Efetov, Phys. Rev. Lett. **97**, 236801 (2006).
[16] P. M. Ostrovsky, I. V. Gornyi, and A. D. Mirlin, Phys. Rev. B **74**, 235443 (2006).
[17] S. Liu, T. Ohtsuki, and R. Shindou, Phys. Rev. Lett. **116**, 066401 (2016).
[18] S. Bera, J. D. Sau, and B. Roy, arXiv:1507.07551.
[19] B. Sbierski, E. J. Bergholtz, and P. W. Brouwer, Phys. Rev. B **92**, 115145 (2015).
[20] J. H. Pixley, P. Goswami, and S. Das Sarma, arXiv:1505.07938v2.
[21] A. Schuessler, P. M. Ostrovsky, I. V. Gornyi, and A. D. Mirlin, Phys. Rev. B **79**, 075405 (2009).
[22] W. Wetzel, Phys. Lett. B **153**, 297 (1985).
[23] A. W. W. Ludwig, Nucl. Phys. B **285**, 97 (1987).
[24] C. Luperini and P. Rossi, Ann. Phys. **212**, 371 (1991).
[25] A. Bondi, G. Curci, G. Paffuti, and P. Rossi, Ann. Phys. **199**, 268 (1990).
[26] N. D. Tracas and N. D. Vlachos, Phys. Lett. **236**, 333 (1990).
[27] A. W. W. Ludwig and K. J. Wiese, Nucl. Phys. B **661**, 577 (2003).
[28] K. B. Efetov, *Supersymetry in Disorder and Chaos* (Cambridge University Press, New York, 1999).
[29] A. Kamenev, *Field Theory of Non-Equilibrium Systems* (Cambridge University Press, New York, 2011).
[30] D. Belitz and T. R. Kirkpatrick, Rev. Mod. Phys. **66**, 261 (1994).
[31] H. B. Nielsen and M. Ninomiya, Nucl. Phys. B **185**, 20 (1981).
[32] M. E. Peskin and D. V. Schroeder, *An Introduction To Quantum Field Theory* (Addison-Wesley, New York, 1975).
[33] B. Sbierski, G. Pohl, E. J. Bergholtz, and P. W. Brouwer, Phys. Rev. Lett. **113**, 026602 (2014).
[34] H. Shapourian and T. L. Hughes, Phys. Rev. B **93**, 075108 (2016).
[35] J. T. Chayes, L. Chayes, D. S. Fisher, and T. Spencer, Phys. Rev. Lett. **57**, 2999 (1986).
[36] A. B. Harris, J. Phys. C **7**, 3082 (1974).
[37] J. H. Pixley, P. Goswami, and S. Das Sarma, Phys. Rev. B **93**, 085103 (2016).
[38] B. Roy and S. Das Sarma, Phys. Rev. B **93**, 119911 (2016).
[39] A. A. Abrikosov, L. P. Gorkov, and I. E. Dzyaloshinski, *Methods of Quantum Field Theory in Statistical Physics* (Dover, New York, 1975).